Raman evidence for orbiton-mediated multiphonon scattering in multiferroic TbMnO$_3$

# Raman evidence for orbiton-mediated multiphonon scattering in multiferroic TbMnO₃

**Pradeep Kumar**[1]**, Surajit Saha**[1]**, D V S Muthu**[1]**, J R Sahu**[2]**,
A K Sood**[1,2] **and C N R Rao**[2]

[1] Department of Physics, Indian Institute of Science, Bangalore-560012, India
[2] Chemistry and Physics of Materials Unit and International Centre for Materials Science,
Jawaharlal Nehru Centre for Advanced Scientific Research, Bangalore-560064, India

E-mail: asood@physics.iisc.ernet.in

**Abstract**
Temperature-dependent Raman spectra of TbMnO₃ from 5 to 300 K in the spectral range of
200–1525 cm⁻¹ show five first-order Raman allowed modes and two high frequency modes.
The intensity ratio of the high frequency Raman band to the corresponding first-order Raman
mode is nearly constant and high ($\sim$0.6) at all temperatures, suggesting an orbiton–phonon
mixed nature of the high frequency mode. One of the first-order phonon modes shows
anomalous softening below $T_N$ ($\sim$46 K), suggesting a strong spin–phonon coupling.

(Some figures in this article are in colour only in the electronic version)

## 1. Introduction

The effect of orbital ordering on the Raman spectra of perovskite manganites, RMnO₃ (R = rare earth), has been investigated both theoretically [1–4] and experimentally [3, 5–8]. Three broad bands near 1000, 1170 and 1290 cm⁻¹ in the Raman spectra of LaMnO₃ were attributed to orbiton excitations [3, 9], an assignment still being debated and alternative proposals made [1, 2, 4, 10]. Although in centrosymmetric LaMnO₃, Raman modes are not infrared active, infrared absorption [10] shows bands similar to those in the Raman spectra, attributing these features to multiphonon scattering instead of orbital excitations. Allen *et al* [1] have proposed that, as a result of strong electron–phonon coupling, orbitons in LaMnO₃ are self-trapped by the local rearrangement of the lattice and hence multiphonon Raman scattering with intensities comparable to those of the one-phonon Raman modes has been predicted. This arises from the Franck–Condon (FC) process via the self-trapped orbitons, suggesting a mixed character of phonons and orbitons for the high frequency modes. This mixed character has also been shown theoretically by other calculations considering the effects of super-exchange and electron–phonon interactions [11, 4]. The high intensity ratio ($\sim$0.1–0.4) of the second-order modes to their first-order counterparts has been observed experimentally

for LaMnO₃ [5] and RMnO₃ (R = La, Pr, Ho and Y) [6], supporting the theoretical proposal for the mixed nature of the multiphonon bands. On the other hand, a recent room temperature Raman study of RMnO₃ (R = Pr, Eu, Dy, Ho and Y) and O¹⁸ isotopically substituted EuMnO₃ [12] suggests that the high frequency modes are due to second-order scattering involving only Brillouin-zone boundary phonons. All these experimental studies have been carried out at room temperature and above. Our present Raman study looks at multiferroic TbMnO₃ as a function of temperature from 5 to 300 K, covering the spectral range from 200 to 1525 cm⁻¹, and focuses mainly on the temperature dependence of the two high energy excitations observed at 1157 and 1328 cm⁻¹.

TbMnO₃ is orthorhombic (space group *Pbnm*) at room temperature and shows an incommensurate lattice modulation at $T_N$ for sinusoidal antiferromagnetic ordering (with $T_N \sim$ 41 K [13] or $T_N \sim$ 46 K as reported by Bastjan *et al* [14]). Ferroelectric order develops at the incommensurate–commensurate transition temperature $T_{FE} \sim$ 27 K [13]. As the temperature is further lowered, rare earth Tb³⁺ ion spins also order antiferromagnetically at $\sim$7 K [13]. In recent years, the focus in multiferroics has been on the electromagnons i.e. magnons with an electric dipole excited by an applied ac electric field, observed below 100 cm⁻¹ [15–19]. As far as first-order phonons are concerned, it has been shown that in
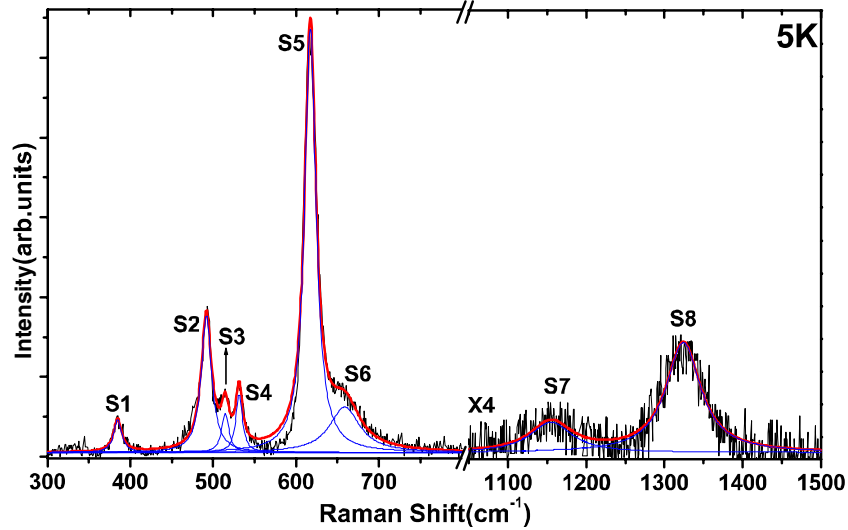
**Figure 1.** Unpolarized Raman spectra of TbMnO$_3$ measured at 5 K. The thick solid line shows the total fit; the thin solid line shows the individual Lorentzian fit.

**Table 1.** List of the experimentally observed phonon frequencies and fitting parameters for a few phonons, fitted using equations (2) and (3) as described in the text. The units are cm$^{-1}$.

| Assignment | Phonon $\omega$ (5 K) | Frequency $\omega$ (0) | $C$ | $\Gamma$(0) | $A$ |
|---|---|---|---|---|---|
| S1 (A$_g$) | 384.9 | 386.1 ± 0.6 | −4.1 ± 0.8 | 10.8 ± 2.7 | 5.9 ± 2.8 |
| S2 (A$_g$) | 491.9 | 495.3 ± 0.3 | −8.5 ± 0.5 | 12.3 ± 0.9 | 10.4 ± 1.4 |
| S3 (A$_g$) | 514.5 | | | | |
| S4 (B$_{2g}$) | 531.3 | | | | |
| S5 (B$_{2g}$) | 616.2 | 620.8 ± 0.7 | −6.2 ± 1.2 | 10.9 ± 1.2 | 14.1 ± 2.1 |
| S6 | 658.4 | 668.8 ± 4.9 | −27.2 ± 8.4 | 40.6 ± 3.2 | 0.09 |
| S7 (second order) | 1157.1 | | | | |
| S8 (overtone) | 1327.4 | | | | |

RMnO$_3$ (R = La, Nd, Sm, Gd, Dy, Pr and Tb), a few Raman and IR phonons involving oxygen vibrations are anomalous, i.e. the phonon frequency decreases as temperature is lowered below $T_N$ [20–23] arising from spin–phonon coupling. There have been reports of Raman studies on multiferroic TbMnO$_3$ dealing with only first-order Raman scattering [20, 24–26], but to our knowledge, there is no report of the high frequency excitations in TbMnO$_3$. In this paper, we present Raman scattering data from an unoriented single crystal of TbMnO$_3$ as a function of temperature in the range 5–300 K. We show that the intensity ratio of the second-order mode to the corresponding first-order one is very high and remains constant with temperature as predicted by Allen *et al* [1, 2] for coupled multiphonon–orbiton modes. In addition, the first-order mode involving oxygen vibrations ($\omega \sim 616$ cm$^{-1}$) shows anomalous softening below $T_N$, possibly due to strong spin–phonon coupling.

## 2. Experimental details

Single crystals of TbMnO$_3$ were grown by the float-zone technique as described in [23]. Confocal unpolarized micro-Raman spectroscopic measurements were performed at low temperatures in backscattering geometry, using a 50× long distance objective and the 514.5 nm line of an Ar ion laser (Coherent Innova 300), covering the spectral range of 200–1525 cm$^{-1}$. Temperature scanning from 5 to 300 K was done using a continuous flow liquid helium cryostat with a temperature accuracy of ±0.1 K. The scattered light was analyzed using a Raman spectrometer (DILOR XY) coupled to a liquid nitrogen cooled CCD, with the pixel resolution of 0.85 cm$^{-1}$ and instrumental broadening of ~5 cm$^{-1}$.

## 3. Results and discussion

Figure 1 shows the Raman spectrum at 5 K displaying eight modes labeled as S1 to S8. The spectra are fitted to a sum of Lorentzians and the frequencies, linewidths and intensities so obtained are shown in figure 2 for the first-order Raman modes and in figure 3 for the multiphonon modes S7 and S8. TbMnO$_3$ is orthorhombic (space group *Pbnm*), with 24 Raman active modes classified as $\Gamma_{Raman} = 7A_g + 5B_{1g} + 7B_{2g} + 5B_{3g}$ [25]. The assignment of the low frequency modes S1–S5, given in table 1, has been done following the work of Iliev *et al* for TbMnO$_3$ [25]. The origin of mode S6 may be similar to that of the 640 cm$^{-1}$ mode observed in LaMnO$_3$ [27, 28], attributed to the disorder-induced phonon density of states [12, 29] or second-order Raman scattering [27]. It can also be a disorder-
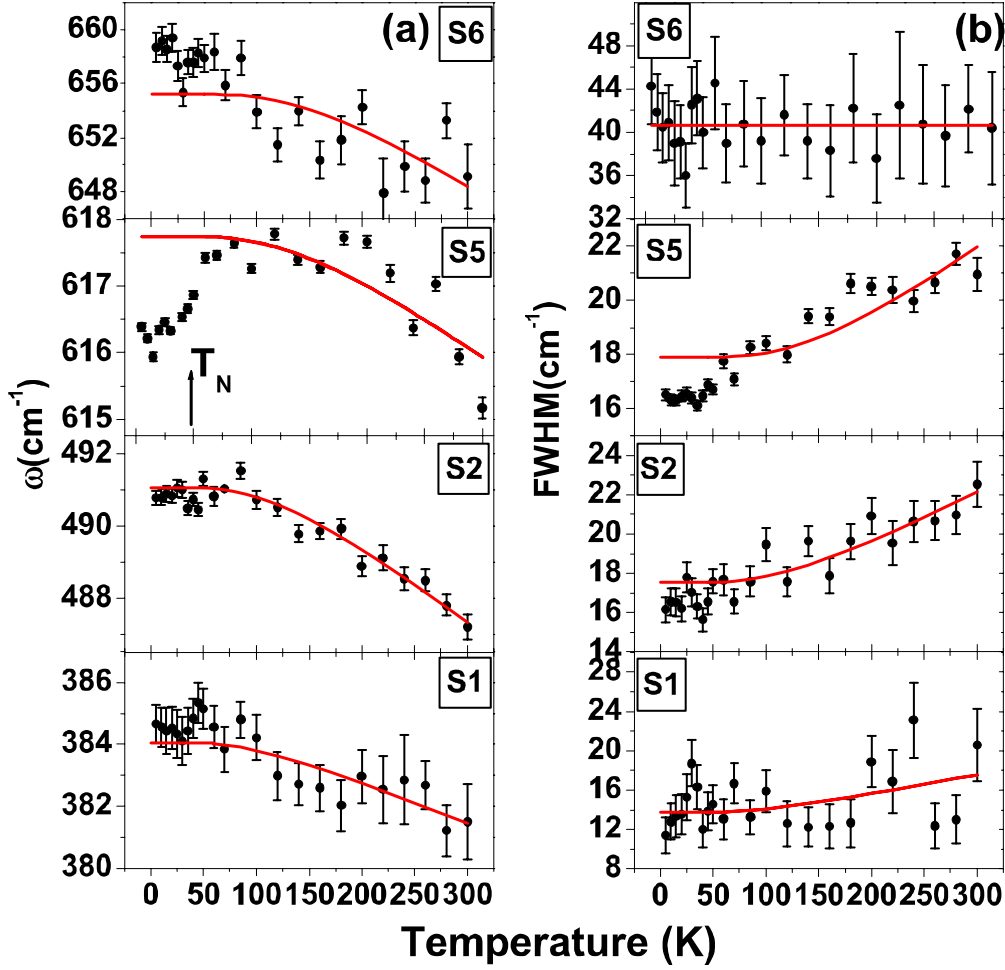
**Figure 2.** Temperature dependence of the modes S1, S2, S5 and S6. The solid lines are the fitted curves as described in the text.

induced infrared active phonon mode (transverse optic mode at 641 cm$^{-1}$ and longitudinal optic mode at 657 cm$^{-1}$) observed in infrared studies of TbMnO$_3$ [23].

### 3.1. Temperature dependence of the first-order modes

We now discuss the temperature dependence of the modes S1 to S5 and S6. In general, the temperature-dependent behavior of a phonon mode of frequency $\omega$ is given as [21]

$$\omega(T) = \omega(0) + (\Delta\omega)_{qh}(T) + (\Delta\omega)_{anh}(T)$$
$$+ (\Delta\omega)_{el-ph}(T) + (\Delta\omega)_{sp-ph}(T). \quad (1)$$

$(\Delta\omega)_{qh}(T)$ corresponds to the change in phonon frequency due to a change in the lattice parameters of the unit cell, termed as the quasi-harmonic effect. $\Delta\omega_{anh}(T)$ gives the intrinsic anharmonic contributions to the phonon frequency. The effect of renormalization of the phonon frequency $((\Delta\omega)_{el-ph}(T))$ due to electron–phonon coupling is absent for insulating TbMnO$_3$. The last term, $\Delta\omega_{sp-ph}(T)$, represents the change in phonon frequency due to spin–phonon coupling, caused by the modulation of the exchange integral by lattice vibrations [21]. The change in phonon frequency of mode $i$ due to the change in lattice parameters, i.e. $(\Delta\omega)_{qh}(T)$, can be related to the change in volume if we know the Grüneisen parameter

$\gamma_i = -(B_0/\omega_i)(\partial\omega_i/\partial P)$, where $B_0$ is the bulk modulus and $\partial\omega_i/\partial P$ is the pressure derivative of the phonon frequency. For a cubic crystal or isotropically expanded lattice, the change in phonon frequency due to the change in volume is given as $(\Delta\omega)_i(T)_{qh}/\omega_i(0) = -\gamma_i(\Delta V(T)/V(0))$. The Grüneisen parameter calculated for RMnO$_3$ (R = Sm, Nd and Pr) is $\sim 2$ [30, 31]. The quasi-harmonic contribution in TbMnO$_3$ can be neglected since the fractional change in volume is negligible [32], as has been done in earlier studies of rare earth manganites RMnO$_3$ (R = Gd, Eu, Pr, Nd, Sm, Tb, Dy, Ho, and Y) [20, 22].

In a cubic anharmonic process, a phonon of frequency $\omega(\vec{\kappa} = 0)$ decays into two phonons, $\omega_1(\vec{\kappa}_1)$ and $\omega_2(\vec{\kappa}_2)$, keeping the energy and momentum conserved, i.e. $\omega = \omega_1 + \omega_2$, $\vec{\kappa}_{1+}\vec{\kappa}_2 = 0$. Considering the simplest decay channel with $\omega_1 = \omega_2$, the temperature dependence of $\omega(T)$ and the full width at half-maximum ($\Gamma$) can be expressed as [33]

$$\omega(T) = \omega(0) + C[1 + 2n(\omega(0)/2)] \quad (2)$$

$$\Gamma(T) = \Gamma(0) + A[1 + 2n(\omega(0)/2)] \quad (3)$$

where $n(\omega) = 1/(\exp(\hbar\omega/\kappa_B T) - 1)$ is the Bose–Einstein mean occupation number and $C$ and $A$ are the self-energy parameters for a given phonon mode. We realize that below
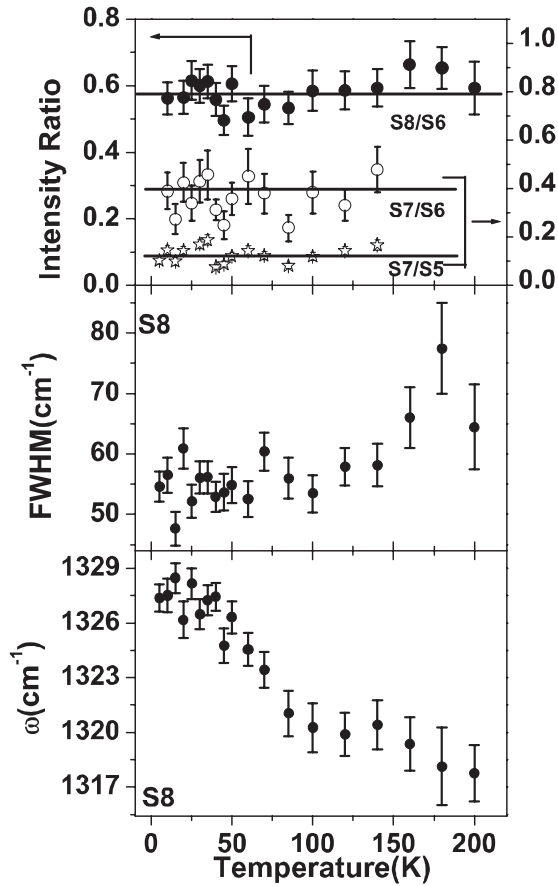
**Figure 3.** Temperature dependence of the intensity ratio of the modes S8 to S6, S7 to S6 and S7 to S5 (top panel). Temperature dependence of the frequency (lower panel) and linewidth (middle panel) of mode S8. Solid lines are a guide to the eye.

the phase transition temperature $T_N$, equations (2) and (3) are not expected to hold good, as is obvious in the temperature dependence of the S5 mode (see figure 2(a)). Therefore, we fit the data between 50 and 300 K using equations (2) and (3) and the theoretical curves are extrapolated below 50 K using the fitted parameters given in table 1 (see the solid lines in figure 2). A similar procedure has been adopted in earlier studies of manganites [20, 22]. We do not observe any significant signature, within the accuracy of our experiments, of the ferroelectric transition at $T_{FE}$ (∼27 K) in the temperature dependence of the frequencies and linewidths. The fit of the data with the Klemens model is modest. The fitting parameter $C$ of mode S6 is very high as compared to those of the other modes, showing that this mode is much more anharmonic. The linewidths and frequencies of the modes S3 and S4 show normal temperature dependence and are not shown here.

An interesting observation is that the intense mode S5 shows anomalous temperature dependence: the mode shows softening near $T_N \sim 46$ K. Similar anomalous temperature dependence has been observed for a few Raman modes in $RMnO_3$ where R = La [21] and Gd, Pr, Nd, Sm, Dy [20, 22], which has been attributed to spin–phonon coupling [21]. This is understood as follows: if an ion is displaced from its equilibrium position by $u$, then the crystal potential is

given as $U = 0.5 \times (ku^2) + \Sigma_{ij} J_{ij}(u) S_i S_j$, where $k$ in the first term represents the force constant and the second term arises from spin interactions between the $Mn^{3+}$ spins. The phonon frequency is affected by the additional term $(\Delta\omega)_{sp-ph}(T) = \lambda\langle S_i S_j\rangle$, where $\lambda = (\partial^2 J_{ij}(u)/\partial u^2)$ is the spin–phonon coupling coefficient and $\langle S_i S_j\rangle$ is the spin-correlation function. The parameter $\lambda$ can be positive or negative and can be different for different phonons. Below $T_N$, the spin correlations build up and hence the spin–phonon coupling becomes important at lower temperatures. The renormalization of the mode S5 frequency starts slightly above $T_N$ (∼ 46 K), which can arise from spin fluctuations due to quantum and thermal effects [20].

### 3.2. Orbiton–phonon coupling

We now discuss the two high energy excitations, S7 at (1157 cm$^{-1}$) and S8 at (1328 cm$^{-1}$). Figure 3 shows the temperature dependence of the frequency and linewidth of the S8 mode as well as the intensity ratio of the S8 and S6 modes (S8/S6) in the temperature range from 5 to 200 K. Above 200 K, the mode S8 is too weak to be analyzed quantitatively, as is the case for S7. Mode S7 can be assigned as the second-order Raman mode involving a combination of S2 and S6 or S4 and S5 phonons and S8 as an overtone of S6 (658 cm$^{-1}$) mode. As the second-order Raman scattering involves the phonons over the entire Brillouin zone, the frequencies of the observed second-order phonons are not necessarily double those of the first-order phonons at the Γ point ($q = (0, 0, 0)$). The intensity ratio of S8 to S6 is most interesting, namely, it is ∼0.6 at all temperatures. The intensity ratio of S7 to S5 is ∼0.1 and that of S7 to S6 is ∼0.4 in the temperature range of 5–140 K. This anomalously large intensity ratio even at low temperatures can only be understood by invoking the mixing of the multiphonon modes with the orbitons [1, 2, 34]. Figure 3 also shows the temperature dependence of the frequency and the linewidth of the S8 mode which has yet to be understood quantitatively for the mixed multiphonon–orbiton mode. It will be interesting to explore the role of spin–charge–lattice coupling in understanding multiphonon Raman scattering in multiferroic $TbMnO_3$. This suggestion arose from the observation of resonance Raman scattering from two magnons in multiferroic $BiFeO_3$ wherein the resonance involves electronic levels, magnons and phonon states [35]. We hope our results will motivate further theoretical studies on this aspect.

## 4. Conclusions

In summary, we have carried out a detailed study of the temperature dependence of the first- and second-order Raman modes of $TbMnO_3$. The intensity ratio of the second-order phonon (S8) to its first-order counterpart (S6) is unusually high and it remains constant down to 5 K. This anomalous temperature dependence of the intensity ratio is attributed to the mixing of the second-order phonon with the orbitons, as theoretically predicted. Four first-order modes (S1, S2, S3 and S4) show normal behavior with temperature, whereas the S5

mode behaves anomalously below $T_N$, this behavior probably arising from a strong spin–phonon coupling. We submit that the present study brings out yet another example of orbiton-mediated multiphonon Raman scattering in the manganite family.

## Acknowledgments

## References

[1] Allen P B and Perebeinos V 1999 *Phys. Rev. Lett.* **83** 4828
[2] Perebeinos V and Allen P B 2001 *Phys. Rev.* B **64** 085118
[3] Saito E, Okamoto S, Takahashi K T, Kobe K, Yamamoto K, Kimura T, Ishihara S, Maekawa S and Tokura Y 2001 *Nature* **410** 180
[4] Vanden Brink J 2001 *Phys. Rev. Lett.* **87** 217202
[5] Kruger R, Schulz B, Naler S, Rauer R, Budelmam D, Backstrom J, Kim K H, Cheong S W, Perebeinos V and Rubhausen M 2004 *Phys. Rev. Lett.* **92** 097203
[6] Martin-Carron L and de Andres A 2004 *Phys. Rev. Lett.* **92** 175501
[7] Choi K Y, Lemmens P, Sahaouri T, Guntherodt G, Pashkevich Y G, Gnezdilov V P, Reutler P, Pinsard-Gaudart L, Bucher B and Revcolevschi A 2005 *Phys. Rev.* B **71** 174402
[8] Choi K Y, Lemmens P, Guntherodt G, Pashkevich Y G, Gnezdilov V P, Reutler P, Gaudart L P, Bucher B and Revcolevschi A 2005 *Phys. Rev.* B **72** 024301
[9] Allen P B and Perebeinos V 2001 *Nature* **410** 155
[10] Gruninger M, Ruckamp R, Windt M, Reutler P, Zobel C, Lorenz T, Freimuth A and Revcolevschi A 2002 *Nature* **418** 39
[11] Bala J, Oles A M and Sawatzky G A 2002 *Phys. Rev.* B **65** 184414
[12] Iliev M N, Hadjiev V G, Litvinchuk A P, Yen F, Wang Y Q, Sun Y Y, Jandl S, Laverdiere J, Popov V N and Gospodinov M M 2007 *Phys. Rev.* B **75** 064303
[13] Kimura T, Goto T, Shintani H, Ishizaka K, Arima T and Tokura Y 2003 *Nature* **426** 55
[14] Bastjan M, Singer S G, Neuber G, Eller S, Aliouane N, Argyrion D N, Cooper S L and Rubhausen M 2008 *Phys. Rev.* B **77** 193105
[15] Pimenov A, Mukhin A A, Ivanov V Y, Travkin V D, Balbashov A M and Loidl A 2006 *Nat. Phys.* **2** 97
[16] Aguilar R V, Sushkov A B, Zhang C L, Choi Y J, Cheong S W and Drew H D 2007 *Phys. Rev.* B **76** 060404
[17] Takahashi Y, Kida N, Yamasaki Y, Fjioka J, Arima T, Shimano R, Miyahara S, Mochizuki M, Furukawa N and Tokura Y 2008 *Phys. Rev. Lett.* **101** 187201
[18] Aguilar R V, Mostovoy M, Sushkov A B, Zhang C L, Choi Y J, Cheong S W and Drew H D 2009 *Phys. Rev. Lett.* **102** 047203
[19] Pimenov A, Shuvaev A, Loidl A, Schrettle F, Mukhin A A, Travkin V D, Ivanov V Yu and Balbashov A M 2009 *Phys. Rev. Lett.* **102** 107203
[20] Laverdiere J, Jandl S, Mukhin A A, Iyanov V Yu, Iyanov V G and Iliev M N 2006 *Phys. Rev.* B **73** 214301
[21] Granado E, Garcia A, Sanjurjo J A, Rettori C, Torriani I, Prado F, Sanchez R D, Caneiro A and Oseroff S B 1999 *Phys. Rev.* B **60** 11879
[22] Ferreira W S, Moreira J A, Almeida A, Chaves M R, Araujo J P, Oliveira J B, Machado Da Silva J M, Sa T M, Mendonca T M, Carvalho P S, Kreisel J, Riberio J L, Vieira L G, Tavares P B and Mendonca S 2009 *Phys. Rev.* B **79** 054303
[23] Kumar P, Saha S, Serrao C R, Sood A K and Rao C N R 2010 *Pramana J. Phys.* **74** 281
Kumar P, Saha S, Serrao C R, Sood A K and Rao C N R 2009 arXiv:0905.3092
[24] Martin-Carron L, de Andres A, Martinez-Lope M J, Casais M T and Alonso J A 2002 *Phys. Rev.* B **66** 174303
[25] Iliev M N, Abrashev M V, Laverdiere J, Jandl S, Gospodinov M M, Wang Y Q and Sun Y Y 2006 *Phys. Rev.* B **73** 064302
[26] Martin-Carron L, Benitz J S and de Andres A 2003 *J. Solid State Chem.* **171** 313
[27] Podobedov V B, Weber A, Romero D B, Rice J P and Drew H D 1998 *Phys. Rev.* B **58** 43
[28] Abrashev M V, Litvinchuk A P, Iliev M N, Meng R L, Popov V N, Ivanov V G, Chakalov R A and Thomsen C 1999 *Phys. Rev.* B **59** 4146
[29] Iliev M N, Abrashev M V, Popov V N and Hadjiev V G 2003 *Phys. Rev.* B **67** 212301
[30] Choithrani R, Gaur N K and Singh R K 2009 *J. Alloys Compounds* **480** 727
[31] Choithrani R, Gaur N K and Singh R K 2008 *J. Phys.: Condens. Matter* **20** 415201
[32] Meier D, Aliouane N, Argyriou D N, Mydosh J A and Lorenz T 2007 *New J. Phys.* **9** 100
[33] Klemens P G 1966 *Phys. Rev.* **148** 845
[34] Cardona M (ed) 1982 *Light Scattering in Solids II* (*Topics in Applied Physics* vol 50) (Berlin: Springer)
[35] Ramirez M O, Kumar A, Denev S A, Chu Y H, Siedel J, Martin L W, Yang S-Y, Rai R C, Xue X S, Ihlefeld J F, Podraza N J, Saiz E, Lee S, Klug J, Cheong S W, Bedzyk M J, Auciello O, Schlom D G, Orenstien J, Ramesh R, Musfeldt J L, Litvinchuk A P and Gopalan V 2009 *Appl. Phys. Lett.* **94** 161905